




Original Article

Fabrication of Decellularized Amnion and Chorion Scaffolds to Develop Bioengineered Cell-Laden Constructs

CHANDRAKALA LAKKIREDDY,¹ SANDEEP KUMAR VISHWAKARMA,¹ NAGARAPU RAJU,¹ SHAIK IQBAL AHMED,¹ AVINASH BARDIA,¹ MAZHARUDDIN ALI KHAN,² SANDHYA ANNAMANENI,³ and ALEEM AHMED KHAN ¹

¹Central Laboratory for Stem Cell Research & Translational Medicine, Centre for Liver Research and Diagnostics, Deccan College of Medical Sciences, Kanchanbagh, Hyderabad, Telangana 500058, India; ²Department of Orthopedics, OHRC, Deccan College of Medical Sciences, Kanchanbagh, Hyderabad, Telangana, India; and ³Department of Genetics, Osmania University, Hyderabad, Telangana, India

(Received 23 March 2021; accepted 15 September 2021; published online 24 September 2021)

Associate Editor Michael R. King oversaw the review of this article.

Abstract

Introduction—Human mesenchymal stem cells (hMSCs) holds great promise for managing several clinical conditions. However, the low engraftment efficiency and obscurity to harvest these cells without compromising the cellular viability, structural and functional properties from the culture niche still remain major obstacles for preparing intact regenerative constructs. Although few studies have demonstrate different methods for generating cell-liberated amniotic scaffolds, a common method for producing completely cell-liberated amnion (D-HAM) and chorion (D-HCM) scaffolds and their cytocompatibility with hMSCs yet to be demonstrated.

Methods—A common process was developed for preparing D-HAM and D-HCM scaffolds for assessing hMSCs engraftment efficiency, proliferation and molecular shifts to generate cell-laden biological discs. The structural and functional integrity of D-HAM and D-HCM was evaluated using different parameters. The compatibility and proliferation efficiency of hMSCs with D-HAM and D-HCM was evaluated.

Results—Histological analysis revealed completely nucleic acid-free D-HAM and D-HCM scaffolds with intact extracellular matrix, mechanical and biological properties almost similar to the native membranes. Human MSCs were able to adhere and engraft on D-HCM better than D-HAM and expanded faster. Ultrastructural observations, crystal violet staining and expression studies showed better structural and

functional integrity of hMSCs on D-HCM than D-HAM and control conditions.

Conclusion—A common, simple and reliable process of decellularization can generate large number of cell-liberated amniotic scaffolds in lesser time. D-HCM has better efficiency for hMSCs engraftment and proliferation and can be utilized for preparing suitable cell-laden constructs for tissue engineering applications.

Keywords—Amniotic scaffolds, Decellularization, Mesenchymal stem cells, Bioengineered constructs.

INTRODUCTION

Biofabrication of tissue specific functional constructs has always been challenging for successful clinical applications.^{3, 6} Biofabrication approach initially requires an appropriate scaffold encompassing crucial biomimetic properties such as cytocompatibility, biodegradability, non-immunogenicity, and three-dimensional architecture of extracellular matrix (ECM) components similar to the native tissues or organs. Further, an appropriate cell source is essential with ease of wider availability and less ethical hurdles encompassing non-immunogenicity, non-tumorigenicity, multipotent potential and enhanced regenerative ability for bioengineering functional constructs.

The earlier biofabrication strategies using natural, synthetic, and 3D-printed scaffolds have failed to provide desired niche for enhanced engraftment, survival and long-term function of cells.³ Cultured cells on scaffolds should be immunologically tolerable suitable for preparing ready to use biological constructs without distressing morphological and functional

Address correspondence to Aleem Ahmed Khan, Central Laboratory for Stem Cell Research & Translational Medicine, Centre for Liver Research and Diagnostics, Deccan College of Medical Sciences, Kanchanbagh, Hyderabad, Telangana 500058, India. Electronic mail: aleem_a_khan@rediffmail.com

Chandrakala Lakkireddy and Sandeep Kumar Vishwakarma share equal first authorship for this manuscript.

properties of cells as well as scaffolds. Therefore, preservation of cell to cell and cell to ECM is essential to generate functionally active biological constructs for wider applicability. Compared to metallic and polymer scaffolds, native tissue derived cell-liberated scaffolds generated by decellularization approach have proved better to convene the above criterias. Scaffolds generated from xenogeneic and allogeneic sources pretense limited availability, immunogenicity, and transfer of infectious or zoonotic diseases.³⁸ Hence, there is a need to identify more appropriate source with a reproducible processing strategy for generating ECM scaffolds and a suitable source of human cells for practical biofabrication strategies.

Decellularized human amniotic membranes (D-HAMs) are gaining much attention in regenerative medicine as an ideal scaffold to biofabricate functional biological constructs. The process of decellularization involves the removal of cells maintaining the natural 3D-structural architecture and biochemical composition of a naïve tissue or organ, making it free of immune components and generating a scaffold compatible for cell adherence and proliferation.^{12,38,41,45}

The earlier approaches of decellularization have demonstrated either complete amniotic membrane or confusing reference to amniotic scaffolds and importance of chorion has not been explored in detail.^{20,31,33,42} Amniotic membranes are comprised of two different types of membranes referred as amnion and chorion. Amnion has been used in numerous regenerative therapies either directly in their naïve form followed by simple washing steps or in other processed forms like denuded, and lyophilized form, ECM protein extracts, decellularized membrane grafts and cell-laded implants.^{8,13,17,19,51} Both amnion and chorion membranes are the richest sources of cytokines and growth factors.^{30,53} Therefore, decellularized amniotic ECM components have been used to promote cellular differentiation.¹³ All these properties make amniotic membranes a suitable biomaterial for generating appropriate biological scaffolds for biofabricating high-grade functional constructs. However, a commonly applicable and reliable method to simultaneously generate completely cell-liberated and immunologically tolerable amnion (D-HAM) and chorion (D-HCM) scaffolds has not been explored yet. Further, comparative cytocompatibility and preserved structural and functional integrity of cell-laden D-HAM and D-HCM need to be compared to predict better choice for preparing suitable biological constructs.

In this study, a common, efficient, reliable and simple cell-liberation process has been developed for producing non-immunogenic D-HAM and D-HCM

with minimal use of detergents. As the success of biofabrication approaches rely on identifying suitable cell source, several studies have reported the beneficial clinical outcomes using MSCs in pre-clinical and clinical settings.^{16,48} Hence, we used human umbilical cord blood (UCB) as a non-invasive and biological waste source^{24,49} to derive mesenchymal stem cells (MSCs) for generating biological constructs using D-HAM and D-HCM scaffolds. The comparative analysis of cell-laden D-HAM and D-HCM has been investigated using detailed histological, ultra-structure and molecular investigations.

MATERIALS AND METHODS

This study has been approved by the Institutional Review Board (IRB), Deccan College of Medical Sciences, Hyderabad, Telangana, India. Signed informed consent forms were collected from each study participant prior to sample collection and clinical history was obtained to determine chromosomal abnormalities or any potent infection. All the study participants were women of age between 23 to 28 years.

Sample Collection and Transportation

Human placenta ($n = 6$) and umbilical cord blood (UCB, $n = 6$) samples were obtained from the Department of Gynecology, Owaisi Hospital and Research Centre, Hyderabad, Telangana, India. Placenta were collected in sterile conditions post-cesarean from healthy female subjects and transported to the sample processing room in normal saline containing antibiotics and antimycotics.

Generation of D-HAM and D-HCM Scaffolds Using a Common Decellularization Process

Each placental tissue was used for separation of amniotic membranes from other components of the tissue through blunt dissection. Afterwards amnion and chorion were separated manually from each other while immersed in saline in a class II biosafety cabinet. Both the amniotic membranes were washed twice with $1 \times$ phosphate buffer saline (PBS) and termed as fresh human amniotic (F-HAM) and chorionic (F-HCM) membranes. Both the membranes were further subjected to a common detergent-based decellularization process.

Both F-HAM and F-HCM were kept separately in sterile closed containers. An increasing gradient of sodium dodecyl sulfate (SDS) was used for incubation in 0.1% for 12 h, 0.5% for 12 h and 1% for 6 h sequentially to remove cells and nuclear materials on

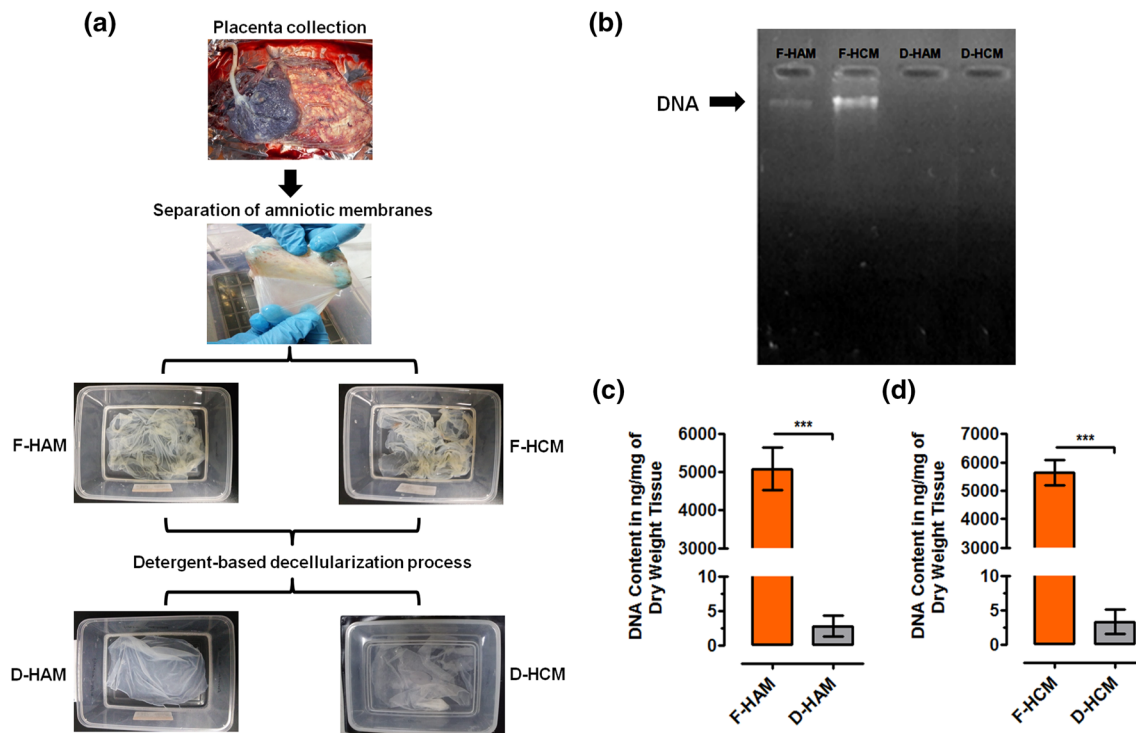


FIGURE 1. (a) Representative optical images showing steps involved in decellularization process of amniotic membranes (amnion and chorion). (b) Qualitative analysis of DNA in D-HAM and D-HCM by agarose gel electrophoresis reveal complete absence of DNA after decellularization process. (c) Quantitative analysis of DNA shows significantly reduced quantity in D-HAM compared to F-HAM ($***p = 0.0001$) and similarly. (d) D-HCM shows significantly reduced quantity of DNA compared to F-HCM ($***p = 0.0001$).

continuous shaking at 60rpm in an incubator at 37 °C temperature. These membranes were then incubated for 2 h in 0.5% Triton-X 100 to remove residual deoxyribonucleic acid (DNA). To ensure complete removal of cellular components, residual detergents and chemical components, a terminal incubation was carried out in 0.1 N NaOH solution followed by 3–5 washes using 1× PBS. Terminal sterilization was carried out for 15 min by exposing D-HAM and D-HCM to ultra-violet (UV) radiation.

Determining Decellularization Efficiency Using Qualitative and Quantitative Assessment of Residual Nucleic Acids

DNA was extracted from 100 mg tissue of amnion and chorion pre- and post-decellularization process. Agarose gel electrophoresis was used for qualitative assessment of DNA in D-HAM, and D-HCM compared to F-HAM, F-HCM. A total of 2 μ L DNA was loaded in 1% agarose gel to determine the decellularization efficiency of both membranes. Further, quantitative assessment was used to measure the quantity of DNA present in per milligram of tissue using nanodrop reading (Thermo Scientific, USA).

Histological Evaluation of D-HAM and D-HCM

Histology of D-HAM and D-HCM was done to evaluate the absence of nuclei and maintenance of ECM integrity in D-HAM and D-HCM compared to F-HAM and F-HCM. For histological analysis, each sample was fixed in 4% paraformaldehyde and further dehydrated using gradients of ethanol and finally embedded in paraffin blocks. Thin sections of 4–5 μ m of each block was prepared and fixed on individual slides. Each section was stained with hematoxylin and eosin (H&E), Sirius red, Masson trichrome, and Alcian Blue to assess effectiveness of the decellularization process. Stained images were documented using Axiovert version 4.2 software in an inverted fluorescence microscopy (Carl Zeiss, Germany).

Cells Isolation, Viability Assessment, and Counting

Human UCB sample (30 mL) was collected in heparin containing sterile 50 mL tube from healthy female subjects during cesarean. Mononuclear cells (MNCs) were isolated using ficoll-paque density gradient centrifugation within 60 min of collection. Briefly, diluted hUCB sample (1:1) was layered on ficoll-paque and centrifuged at 3000 rpm for 45 min.

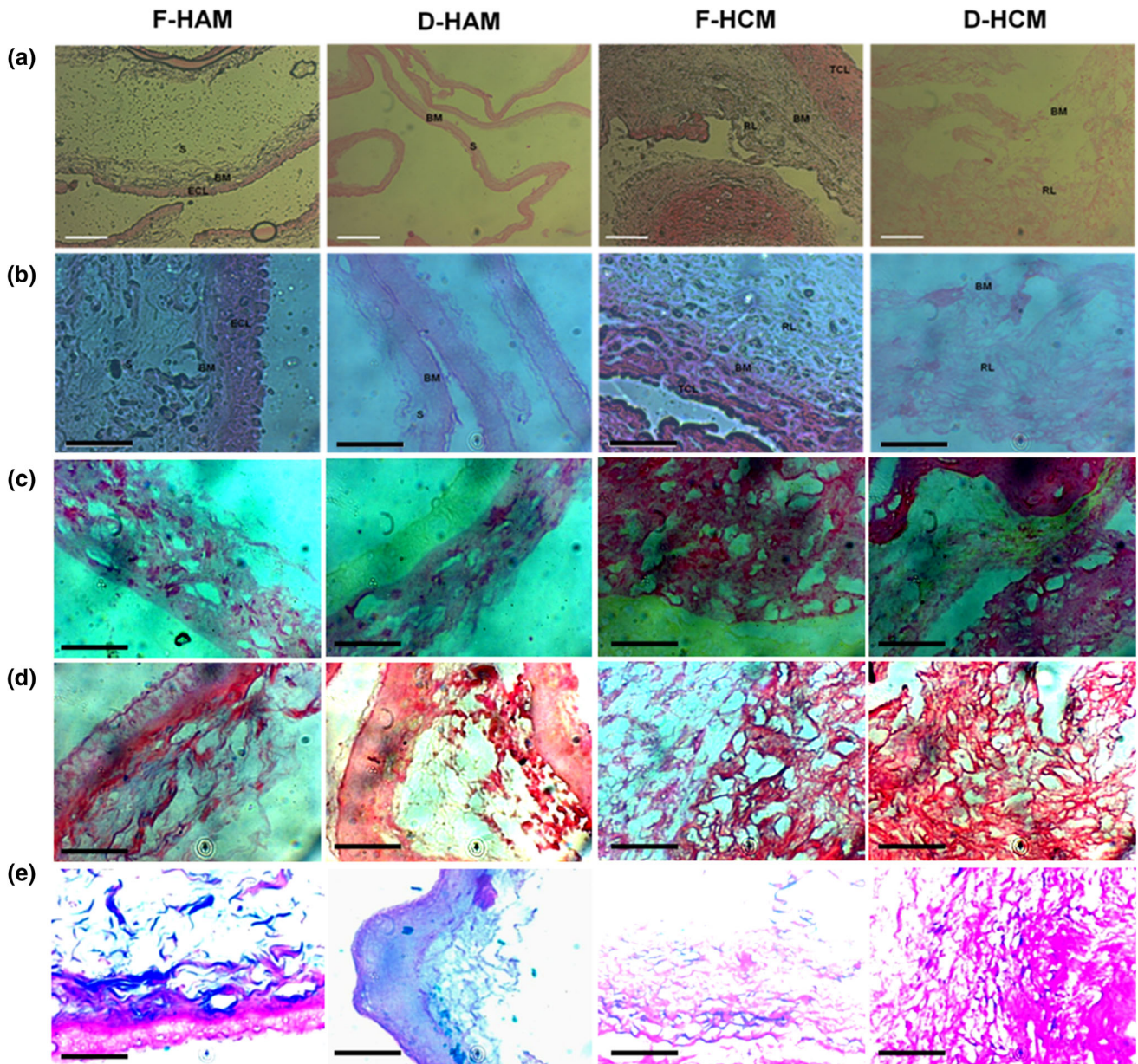


FIGURE 2. Histological analysis of H&E stained sections of fresh and decellularized membranes reveals complete removal of epithelial cell layer and trophoblast cell layer in D-HAM and D-HCM after decellularization process. (a) $\times 10$ magnification, scale bar $100\ \mu\text{m}$. (b) $\times 40$ magnification, scale bar $50\ \mu\text{m}$. In contrast, it is visible from the stained sections that F-HAM and F-HCM containing a well distinguished epithelial and trophoblast cell layers. After the decellularization process, D-HAM and D-HCM preserve the ECM, and a complete absence of nuclei can be seen in both D-HAM and D-HCM. (c) Sirius red staining showed no significant change in the distribution and quantity of collagen after decellularization. (d) Masson trichrome staining showing intact appearance of collagen and elastin with no obvious disruptions to collagen and elastin after decellularization. (e) Alcian Blue pH-1 staining demonstrated conserved GAGs after decellularization as compared to fresh membranes. ECL, Epithelial Cell Layer; BM, Basement Membrane; S, Stroma; TCL, Trophoblast Layer; RL, Reticular Layer.

Middle buffy-coat layer containing mononuclear cells (MNCs) was collected and washed with $1\times$ PBS by centrifugation at 3000 rpm for 15 min.

MNCs were assessed for viability using Trypan blue exclusion and fluorescein diacetate (FDA) assays and counted using hemocytometer. Briefly, human UCB-MNCs were stained with 0.2% trypan blue for

checking viability percentage and cell number using following formula:

$$\text{Percentage cell viability} = (\text{number of viable cells}/\text{total number of cells}) \times 100$$

$$\text{Dilution factor (DF)} = \text{Total volume}/\text{volume of hUCB - MNCs}$$

$$\text{Total number of cells/mL} = \text{Average number of cells per square} \times \text{DF} \times 10^4$$

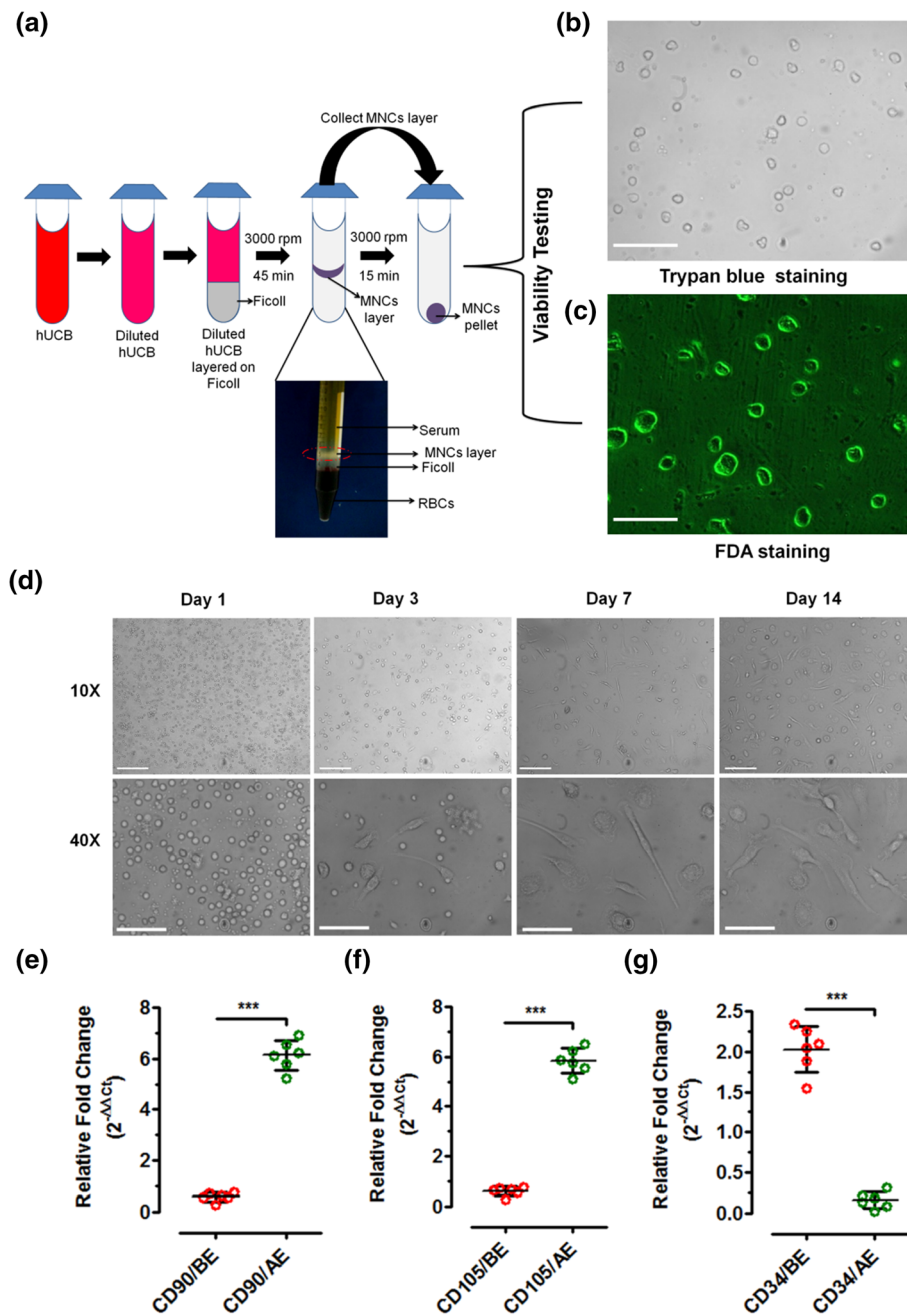


FIGURE 3. (a) Schematic representation of MNCs isolation from hUCB followed by viability testing using Trypan blue staining (×40 magnification, scale bar 20 μm) and FDA staining (×40 magnification, scale bar 20 μm, at day 1 scale bar 50 μm). (b) Morphometric observation of 2D-enriched hUCB-MSCs from day 1 to day 14. Microscopic observation reveals that from day 3, hUCB-MSCs started showing their characteristic fibroblast morphology, and by day 14, they reach to 80% confluency (×10 magnification, scale bar 100 μm, ×40 magnification, scale bar 20 μm); Gene expression analysis of 2D-enriched hUCB-MSCs using positive and negative gene transcripts show significantly increased levels for CD90 and CD105 and reduced for CD34 (*** $p = 0.0001$).

For FDA assay, 1.0×10^6 hUCB-MNCs were taken in a 1.5 mL microcentrifuge tube and incubated with 5 μL of 1 μg/mL FDA solution for 5 min at room temperature. FDA stained hUCB-MNCs were washed

twice with $1 \times$ PBS and mounted on a microscopic glass slide. These slides were visualized under an inverted fluorescence microscope (Carl Zeiss, Germany) and documented using Axiovert software.

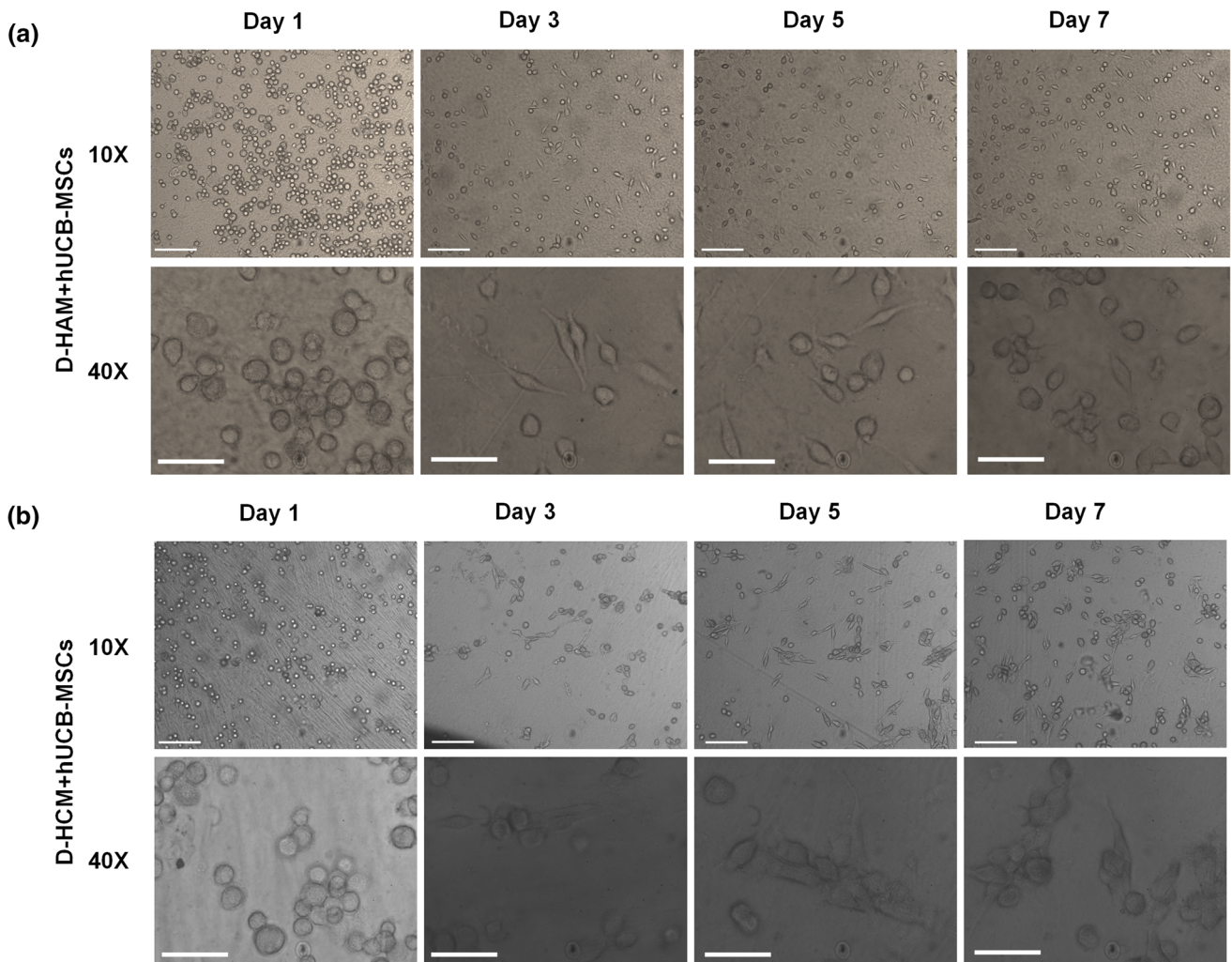


FIGURE 4. (a) Morphometric characterization of 2D-enriched hUCB-MSCs cultured on (a) D-HAM; (b) D-HCM. Both D-HAM and D-HCM support the adherence and proliferation of hUCB-MSCs ($\times 10$ magnification, scale bar $100\ \mu\text{m}$, $\times 40$ magnification, scale bar $20\ \mu\text{m}$)

In Vitro Enrichment and Passaging of Human MSCs

A total of 3.0×10^6 hUCB-MNCs were cultured in T-25 flask using low glucose Dulbecco's Modified Eagle Medium (DMEM, Gibco) supplemented with 10% fetal calf serum (FCS) containing 100 U/mL Penicillin (Invitrogen), 100 $\mu\text{g}/\text{mL}$ streptomycin (Invitrogen), and 0.25 mg/mL amphotericin B (Invitrogen). Culture flasks were incubated for 48 h in a CO_2 incubator with 5% CO_2 at $37\ ^\circ\text{C}$ in a humidified environment. After 48 h, un-adhered cells were removed and adhered cells were replenished with fresh culture media. The adhered cells were allowed to proliferate further up to 14 days based on the earlier literature and our preliminary experiences. The culture media was replenished every 3 days to remove dead cells and their toxic products during 14 days of enrichment process.

Enriched MSCs were trypsinized at day 14 and sub-cultured up to 6–8 passages. Briefly, the culture media was removed completely from the adherent MSCs monolayer in T-25 flasks and washed once with $1\times$ PBS. Further, cells were incubated in 3 mL of $1\times$ trypsin-EDTA for 10 min in a CO_2 incubator at 37°C for detaching the cells from the culture flasks. After retrieving cells from the culture flasks, desired amount of medium was added into each flask and cells were collected in 15 mL falcon tubes. The cell suspension was centrifuged at 2000 rpm for 10 min and cells pellet was washed with $1\times$ PBS. Finally MSCs were suspended in culture medium and assessed for viability before passaging.

Characterization of hUCB-MSCs Enrichment

Morphometric characterization was done using confocal microscopy observation of hUCB-MSCs at day 1, 3, 7, and 14.

Gene expression analysis of MSCs before (BE) and after enrichment (AE) was conducted using quantitative real-time polymerase chain reaction (RT-qPCR) by extracting total ribonucleic acid (RNA) followed by construction of complementary DNA (cDNA). Briefly, enriched MSCs at day 14 were trypsinized and harvested for isolating RNA using guanidinium isothiocyanate (GITC) method as described earlier.⁴ RNA quantity was measured using nanodrop readings. For cDNA construction, 1 μ g of RNA was used using oligo dT primer and reverse transcriptase II enzyme (Fermentas). SYBR-Green assay was performed for the quantification of relative expression of each selected gene transcripts. Gene specific forward and reverse primers were used to carry out the transcript quantification as follows: positive gene transcripts CD90 (Forward primer: 5'-GGGTTGGA-GAAGGAGGTAAAG-3'; Reverse primer: 5'-CGCAGAAGTCCCTGAGAAG-3'), and CD105 (Forward primer: 5'-CCACTAGCCAGGTCTC-GAAG-3'; Reverse primer: 5'-GATGCAGGAAG-CACTGCTG-3'), negative gene transcript CD34 (Forward primer: 5'-CTACAA-CACCTAGTACCCTTGGGA-3'; Reverse primer: 5'-GGTGAACACTGTGCTGATTACA-3') and reference gene transcript GAPDH (Forward primer: 5'-GAAGGTGAAGGTCGGAGTC-3'; Reverse primer: 5'-GAAGATGGTGATGGGATTTTC-3'). Each reaction was carried out in triplicates for each sample to avoid any technical error.

Biofabrication of Cell-Laden Disk-Shaped Constructs Using D-HAM and D-HCM

D-HAM and D-HCM were cut into 4 cm patches and placed carefully on 40 mm plastic coverslips using blunt end forceps. These coverslips containing D-HAM and D-HCM scaffold disks were placed in each well of a six-well plate. Before hUCB-MSCs seeding, these scaffolds were sterilized for 15 min, and preconditioned with culture media for 12 h.

Human UCB-MSCs (0.4×10^6 cells per disk) from 2-5 passages were seeded on D-HAM and D-HCM scaffold disks for cytocompatibility assessment in time-dependent manner. Morphometric characterization was performed using microscopic observation to identify the adherence and proliferation of hUCB-MSCs on D-HAM and D-HCM scaffolds at regular time-intervals from day 1 to day 7.

Crystal violet staining was done to determine the morphology of MSCs at day 7 as described earlier.²⁷ Briefly, the hUCB-MSCs were fixed using 4% paraformaldehyde for 10 min at room temperature, and washed with $1 \times$ PBS. Human UCB-MSCs were then stained with 1% crystal violet and incubated for 10 min at room temperature. Incubation was followed by washing steps to remove the excess stain. D-HAM and D-HCM scaffold disks were allowed to dry prior to microscopic observation.

The ultrastructural analysis of hUCB-MSCs on D-HAM and D-HCM was performed at day 7 after culture using scanning electron microscopy (SEM) to determine the structural integrity and interactions of MSCs and scaffolds. Biofabricated D-HAM and D-HCM scaffolds were fixed in 2.5% glutaraldehyde and processed for SEM analysis using protocol as described earlier.²

Cell Viability Assessment and Transcript Analysis for Cell-Laden D-HAM and D-HCM Constructs

MTT 3-(4,5-dimethylthiazol-2-yl)-2,5-diphenyltetrazolium bromide) assay was performed to identify the cytocompatibility of D-HAM and D-HCM by assessing the viability of hUCB-MSCs at day 1, 3, 5, and 7. 2D-cultured MSCs directly on plastic surfaces were maintained as control group along with hUCB-MSCs on D-HAM and D-HCM. Briefly, at the end of each time point, 300 μ L of 2 mg/mL MTT was added into each group (present in a single well of a 6-well plate) and incubated for 4 h. After incubation in each group, 300 μ L of DMSO was added to stop the MTT reaction and incubated all groups for 10 min. Optical density (OD) of hUCB-MSCs was taken at 540-570 nm using a microplate reader.

Further, validation of D-HAM and D-HCM scaffolds cytocompatibility was assessed through gene expression analysis at day 7 after culture using RT-qPCR for MSCs positive gene transcripts (CD90 and CD105) and negative transcript (CD34) by extracting RNA from biofabricated D-HAM and D-HCM followed by cDNA construction as described earlier.

Statistical Analysis

Statistical analysis was performed by using GraphPad Prism (Version 5). Unpaired *t* test, one-way and two-way ANNOVA parametric tests were used, followed by D'Agostino and Pearson omnibus normality test and Bonferroni posttests. $p \leq 0.05$ was considered to be statistically significant for all the groups.

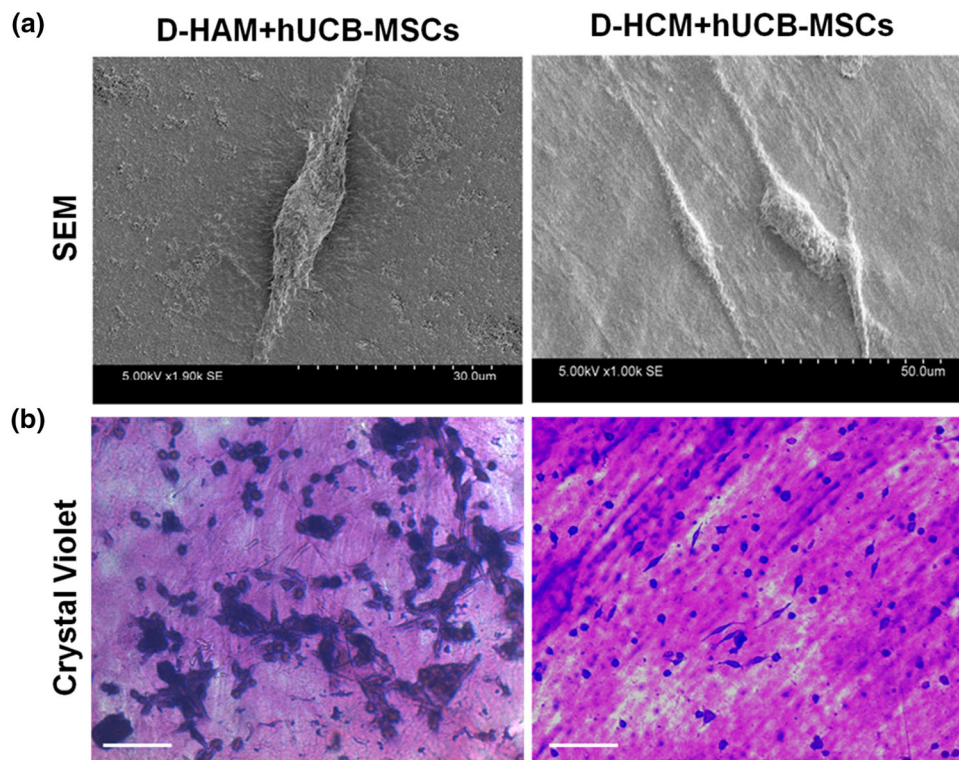


FIGURE 5. (a) SEM analysis revealed that hUCB-MSCs show characteristic flattened spindle-shaped morphology with elongated extensions and a well-established interactions with cell to cell and matrix on both D-HAM and D-HCM; (b) Crystal violet staining of hUCB-MSCs on D-HAM and D-HCM, hUCB-MSCs stained in purple colour and maintain their characteristic fibroblast morphology ($\times 10$ magnification, scale bar 100 μm).

RESULTS

Biofabrication of D-HAM and D-HCM

Separation of amniotic membranes from placenta was carried out by blunt end dissection. Amnion and chorion were separated physically and exposed to the detergent-based decellularization process individually. Optical observation revealed that D-HAM and D-HCM appeared more translucent than F-HAM and F-HCM, suggesting a loss in cellular components after the complete decellularization process. No visible loss was noted in the ECM architecture of D-HAM and D-HCM, signifying the retention of 3D-ECM structural integrity (Fig. 1a).

The efficiency of the decellularization process was evaluated both qualitatively and quantitatively before and after decellularization. Qualitative assessment of residual DNA in D-HAM and D-HCM by agarose gel electrophoresis revealed a complete absence of DNA, indicating that the process of decellularization effectively removed DNA from F-HAM and F-HCM (Fig. 1b). These results were validated further by quantitative analysis by measuring the amount of DNA using nanodrop reading at 260/280 nm in DNA isolated from F-HAM, F-HCM, D-HAM, and D-HCM. Results show significant decrease

($***p = 0.0001$) in the amount of DNA in both D-HAM (2.767 ± 1.521) and D-HCM (3.317 ± 1.768) compared to F-HAM (5083 ± 564.4) and F-HCM (5649 ± 442.6) (Figs. 1c and 1d). The DNA quantity was negligible and followed the required decellularization criteria to become non-immunogenic.⁵ This common decellularization process ensures complete removal of cellular and nucleic acid components retaining the ECM integrity and proteins in both the membranes.

Further, identification of cellular, nuclear, and ECM component changes during the pre- and post-decellularization process was performed by histological characterization using H&E, Sirius red, Masson trichrome, and Alcian blue staining. All staining revealed a complete absence of cellular components, nuclei, and retention of 3D-ECM integrity. H&E staining analysis reveals complete removal of epithelial cell layer and nuclei in D-HAM compared to F-HAM (Fig. 2a). Similarly, in D-HCM, the trophoblast cell layer and nuclei are completely absent compared to F-HCM (Fig. 2b). Sirius red staining showed a well integrated collagen (Fig. 2c). Masson trichrome staining showed intact collagen and elastin ECM components of both D-HAM and D-HCM compared to fresh membranes (Fig. 2d). Alcian blue staining showed intact distribu-

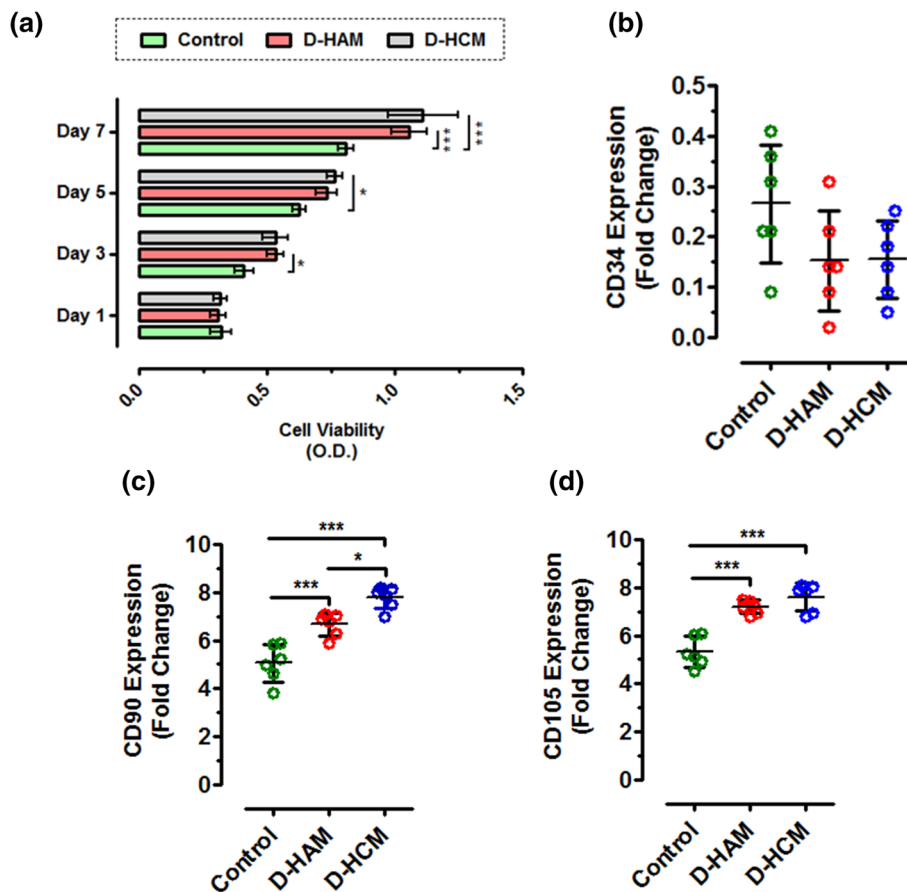


FIGURE 6. (a) Viability assessment of hUCB-MSCs on D-HAM and D-HCM showed a significant increase in the viability of hUCB-MSCs from day 3 to day 7 in all conditions ($***p = 0.0001$, $*p = 0.01$). Gene expression analysis of hUCB-MSCs cultured on D-HAM and D-HCM shows. (b) No significant difference for CD34 expression between control, and D-HAM and D-HCM ($p > 0.05$), while positive gene transcripts CD90 and CD105 show significant increase in expression levels in D-HAM and D-HCM compared to control ($*p = 0.01$, $***p = 0.0001$).

tion and quantity of glycosaminoglycans (GAGs) post-decellularization (Fig. 2e).

Enumeration of hUCB-MSCs

MNCs isolation was performed using Ficoll-paque density gradient centrifugation (Fig. 3a). Trypan blue and FDA staining was performed for assessing the viability of MNCs. When stained with trypan blue, viable cells with intact cell membrane excluded the dye and appeared colorless (Fig. 3b). Similarly, when stained with FDA viable MNCs with intact membrane emitted green fluoresce due to the action of esterases (Fig. 3c). MNCs were counted using hemocytometer to determine the percentages of cell viability and number of total viable cells. Our results showed more than 95% viability of isolated MNCs.

Before the cytocompatibility assessment of D-HAM and D-HCM, viable MNCs were enriched into MSCs in 2D-*in vitro* culture conditions. The MSCs population present in the cultured MNCs started adhering to

the culture flask within 48 h. Further, morphometric changes in cultured MNCs were monitored regularly at day 1, 3, 7, and 14 under confocal microscopy. Gradual change in morphology was noted from day 3 in adhered MSCs with change in cell shape from spherical to fibroblast. By day 14, MSCs reached 80% confluency in 2D-culture conditions (Fig. 3d). This 2D-enriched MSCs population further maintained *in vitro* 2D-culture conditions by frequent trypsinization and passaging for further experimental analysis.

Gene expression analysis was performed using MSCs positive markers (CD90 and CD105) and negative marker (CD34) before enrichment at day 1 and after enrichment at day 14. Relative quantification of the above gene transcripts showed a significantly higher expression of CD90 AE (6.137 ± 0.5844 ; $***p = 0.0001$) compared to BE (0.5733 ± 0.1719) (Fig. 3e). Similarly, a significant higher expression of CD105 AE (5.840 ± 0.4984 ; $***p = 0.0001$) compared to BE (0.6017 ± 0.178) was identified (Fig. 3f). A significantly decreased expression of CD34 AE

(0.1600 ± 0.1008 ; $***p = 0.0001$) compared to BE (2.028 ± 0.2862) was identified (Fig. 3g).

Comparative Analysis of Cell-Laden D-HAM and D-HCM

Enriched MSCs between 2 and 5 passages were used for assessing the cytocompatibility of D-HAM and D-HCM. These MSCs were used to biofabricate D-HAM and D-HCM disks. Microscopic observation revealed that D-HAM and D-HCM supported the adherence and proliferation of allogenic hUCB-MSCs. Further, it was noted that the hUCB-MSCs reached 80% confluency on D-HAM and D-HCM scaffolds within 7 days (Figs. 4a and 4b). Biofabrication of hUCB-MSCs on D-HAM and D-HCM have better advantages than control condition, since these biofabricated D-HAM and D-HCM can be used for various bioengineering and regenerative applications without disturbing the cell to cell and cell to ECM interactions.

Ultrastructural analysis of biofabricated D-HAM and D-HCM was carried out using SEM analysis to find out hUCB-MSCs morphology, the interaction between the scaffold and cells, and ECM integrity after cellularization at the ultrastructural level. SEM analysis revealed well-established cell to cell and cell to matrix interactions and intact 3D-ECM structural integrity on D-HAM and D-HCM (Fig. 5a). Microscopic observation of crystal violet stained hUCB-MSCs on D-HAM and D-HCM showed flattened fibroblast shaped morphology with lengthened extensions (Fig. 5b).

Further, cytocompatibility assessment of biofabricated D-HAM and D-HCM was validated by evaluating cell viability and gene expression analysis. Viability analysis using MTT revealed an increase in hUCB-MSCs viability from day 3 to day 7 on D-HAM and D-HCM. On day 1, the viability of hUCB-MSCs was almost the same on D-HAM and D-HCM. However, a significant increase in hUCB-MSCs was noted on D-HAM and D-HCM at day 3 ($*p = 0.01$), day 5 ($*p = 0.01$), and day 7 ($***p = 0.0001$) when compared with control hUCB-MSCs (Fig. 6a).

Gene expression analysis of cell-laden D-HAM and D-HCM for MSCs positive markers CD90 and CD105 reported a higher expression of these genes in biofabricated D-HAM and D-HCM when compared with control hUCB-MSCs. CD90 expression was found significantly higher on D-HAM (6.673 ± 0.4742 ; $***p = 0.0001$) and D-HCM (7.790 ± 0.4604 ; $***p = 0.0001$) when compared with control hUCB-MSCs (5.050 ± 0.7950). It was noted that hUCB-MSCs showed significantly higher expression of CD90 on D-HCM ($*p = 0.01$) when compared to D-HAM (Fig. 6c). CD105 expression was found significantly

higher on D-HAM (7.200 ± 0.2775 ; $***p = 0.0001$) and D-HCM (7.607 ± 0.5797 ; $***p = 0.0001$) when compared with control hUCB-MSCs (5.317 ± 0.6370 , Fig. 6d). However, no significant change in expression of CD34 was noted for both the scaffolds compared to control (Fig. 6b) and between D-HAM and D-HCM.

DISCUSSION

Scaffolds encompassing suitable microenvironment and biological niche have recently gained attention for diverse tissue engineering and regenerative applications. In this context, decellularized tissues/organs are being explored extensively to support the adherence, proliferation, and differentiation of different types of cells. These scaffolds should also encompass the biocompatibility and permit cell infiltration to generate functional organs/or tissues.^{14,39} Hence, there is a need to identify a material that can mimic ECM of native human tissue encompassing such crucial properties.^{14,35,52} Studies have explored the successful clinical applications of human amniotic membranes (amnion and chorion)²⁵ due to its biocompatible nature and ease of collection from biomedical waste with less ethical concern. Amniotic membranes contain excellent structural and regenerative components that can promote wound healing/tissue remodeling/regeneration.⁴⁴ These properties of human amniotic membranes encourage its potential use in generating cell-liberated bioscaffolds for different tissue engineering applications.

The direct clinical application of human amniotic membranes in its native form poses several hurdles like variation in growth factors, ECM remodeling regulators, decreased biomechanical stability, increased biodegradation, postoperative contamination and inflammatory reactions.^{7,26,36,47} Native HAM contains mesenchymal and epithelial cells and native HCM contains trophoblast cells, hence direct application of these membranes show slight inflammation.^{1,15,23} Therefore, generation of cell-liberated amnion and chorion scaffolds is recommended to avoid host immune responses. Several decellularization methods using chemicals (ethylenediaminetetraacetic acid [EDTA], and urea, enzymes (trypsin, dispase, and thermolysin, and combination of hypotonic buffers with nucleases (TRIS buffer + EDTA + aprotinin + SDS + DNase + RNase and alkaline (NaOH methods have been attempted previously for generating cell-liberated amniotic membranes.^{42,44,50} However, studies are lacking to a common process for generating intact decellularized human amniotic and chorionic membranes. Developing a common process may provide an opportunity to produce large number

of cell-liberated scaffolds concurrently to increase the use in different clinical applications. Moreover, the applicability of such scaffolds may be enhanced by repopulating with different types of cells depending upon the target tissue or organ.

In this study, we explore a common process for decellularizing amnion and chorion membranes concurrently using increasing gradients of SDS. With current advancements in tools and techniques, it is now possible to evaluate the decellularization efficiency using optical and microscopic observations, histological assays, ECM components staining, DNA analysis (qualitative and quantitative), and ultrastructural analysis.⁴⁴ In our study, optical observation shows increasing in translucency of both F-HAM and F-HCM with the decellularization process, indicating the removal of cellular components. Qualitative and quantitative estimation of DNA confirmed that the developed decellularization process effectively removes double-stranded DNA (dsDNA) from F-HAM and F-HCM and produces nucleic acid-deficient D-HAM and D-HCM (Fig. 1). Similarly, earlier studies have shown reduction in the DNA content from 341 ± 29.60 to $39.38 \pm 4.04 \mu\text{g/mL}$,³⁴ and 341 ± 29.60 to $39 \pm 4.06 \mu\text{g/mL}$ ⁴⁷ after the decellularization procedure for HAM and $6000 \pm 2000 \text{ ng/mg}$ to $10 \pm 5 \text{ ng/mL}$ for HCM.¹⁰ We observed DNA quantity of $5083 \pm 230.4 \text{ ng/mg}$ to $2.767 \pm 0.621 \text{ ng/mg}$ for HAM and $5649 \pm 180.7 \text{ ng/mg}$ to $3.317 \pm 0.7218 \text{ ng/mg}$ for HCM which are comparatively less than the earlier studies. Further histological analysis of D-HAM and D-HCM reveals no impact on ECM structural integrity and its components during and after the decellularization process of both D-HAM and D-HCM as demonstrated by H&E and collagen staining (Fig. 2) and are similar to the earlier studies.^{10,11,22}

The clinical applicability of cell-liberated amniotic scaffolds has been well proven in wound healing and several other applications.^{10,18} However, the crucial insights involved in regenerative mechanisms during exogenous or endogenous cellular interaction with the D-HAM remains elusive. Earlier studies have demonstrated that preserving the ECM components of decellularized scaffolds is essential for promoting proliferation and differentiation of allogenic cells.^{9, 11,43,47} Hence, we assumed that D-HAM and D-HCM must promote the growth of allogenic cells for future regenerative applications. Hence, in present study cytocompatibility of D-HAM and D-HCM was tested through *in vitro* biofabrication with hUCB-MSCs. Human UCB-MSCs were expanded in 2D-cultured conditions and compared with expansion and

enrichment on D-HAM and D-HCM (Fig. 3) using quantitative gene expression analysis for MSCs positive (CD90 and CD105) and negative (CD34) markers at day 7. The gene expression analysis showed a significant increase in CD90 and CD105 expression on D-HCM (95% CI -3.668 to -1.812 ; $p < 0.0001$) and D-HAM (95% CI -2.552 to -0.6950 ; $p < 0.0001$) compared to 2D-culture and no significant change in CD34 expression was observed among the groups. Comparative analysis for enrichment efficiency showed significantly higher for D-HCM compared to D-HAM (95% CI -2.045 to -0.1883 ; $p < 0.01$). This expansion and enrichment analysis provided evidence of the superiority of D-HCM to D-HAM and 2D-culture system conditions. Although few studies have reported enhanced MSCs expansion on D-HAM,^{11,40} the studies showing such effects for D-HCM are rare.¹⁰

Evaluation of D-HAM and D-HCM cytocompatibility was studied by culturing hUCB-MSCs. Biofabricated D-HAM and D-HCM were monitored through microscopic observation at regular intervals for checking adherence and proliferation of hUCB-MSCs (Fig. 4). The ultrastructural analysis of biofabricated D-HAM and D-HCM showed a well-established interaction between cells and ECM on both D-HAM and D-HCM (Fig. 5). Further, crystal violet staining for assessing the cellular morphology of hUCB-MSCs on D-HAM and D-HCM revealed maintenance of characteristic fibroblast morphology. Viability analysis revealed a significantly higher percentage of hUCB-MSCs viability on D-HAM and D-HCM compared to control hUCB-MSCs (Fig. 6). These trends in cellular expansion show similar findings to CD90/CD105 expression with the time. The mechanisms for enhanced cell viability and expansion on D-HAM and D-HCM can be explained by well organized cell to ECM interaction due to natural ECM organization composed of collagen, fibronectin and other crucial growth regulatory chemokines and cytokines.^{37,46} Similar observations have been reported for MSCs from other sources cultured on cell-liberated amniotic scaffolds.^{21,28,29}

The data obtained in this study strongly supports that the developed common decellularization process successfully eliminates the cellular and nuclear components from amnion and chorion. Biofabricated D-HAM and D-HCM supports the proliferation of allogenic hUCB-MSCs. Although better properties are identified for D-HCM, cell-laden constructs using both D-HAM and D-HCM can be used for evaluating their potential application in various clinical conditions including wound healing, and tissue regeneration as demonstrated for D-HAM in earlier studies.^{10,32}

CONCLUSION

The decellularization process adopted in this study proved to be common, simple, efficient, and reliable to generate completely cell-liberated D-HAM and D-HCM scaffolds with preserved structural, mechanical and biological properties of native membranes. Cell-laden D-HCM show better adherence, engraftment and proliferation of human UCB-MSCs compared to D-HAM and control conditions. Thus, D-HCM may be a potential biological niche for biofabricating appropriate functional biological constructs without distressing structural and functional integrity of cells adhered on the scaffolds for direct application.

ACKNOWLEDGMENTS

This study was supported by the grant received from Indian Council of Medical Research (ICMR) in form of Research Associate Fellowship (RA, No. 5/3/8/3/ITR-F/2019-ITR) to Sandeep Kumar Vishwakarma. All authors thank to Owaisi Hospital and Research Centre for material supply.

CONFLICT OF INTEREST

Chandrakala Lakkireddy, Nagarapu Raju, Shaik Iqbal Ahmed, Avinash Bardia, Mazharuddin Ali Khan, Sandhya Annamaneni, and Aleem Ahmed Khan declare that they have no conflict of interest.

CONSENT TO PARTICIPATE

All the participants in the study provided signed inform consent forms prior to the sample collection

CONSENT TO PUBLISH

All the participants in the study agreed for publishing this study

ETHICAL APPROVAL

Institutional Review Board has approved present study

REFERENCES

- ¹Barton, K., D. L. Budenz, P. T. Khaw, and S. C. G. Tseng. Glaucoma filtration surgery using amniotic membrane transplantation. *Investig. Ophthalmol. Vis. Sci.* 42(8):1762–1768, 2001.
- ²Bozzola, J. J., and L. D. Russell. *Electron Microscopy Principles and Techniques for Biologists*, 2nd ed. Sudbury, MA: Jones and Bartlett Publishers, 1998.
- ³Bryksin, A. V., A. C. Brown, M. M. Baksh, M. G. Finn, and T. H. Barker. Learning from nature—novel synthetic biology approaches for biomaterial design. *Acta Biomater.* 10(4):1761–1769, 2014. <https://doi.org/10.1016/j.actbio.2014.01.019>.
- ⁴Chomczynski, P., and N. Sacchi. Single-step method of RNA isolation by acid guanidinium thiocyanate-phenol-chloroform extraction. *Anal. Biochem.* 162:156–159, 1987. <https://doi.org/10.1006/abio.1987.9999>.
- ⁵Crapo, P. M., T. W. Gilbert, and S. F. Badylak. An overview of tissue and whole organ decellularization processes. *Biomaterials.* 32(12):3233–3243, 2011. <https://doi.org/10.1016/j.biomaterials.2011.01.057>.
- ⁶Dan, P., É. Velot, G. Francius, P. Menu, and V. Decot. Human-derived extracellular matrix from Wharton's jelly: an untapped substrate to build up a standardized and homogeneous coating for vascular engineering. *Acta Biomater.* 48:227–237, 2017. <https://doi.org/10.1016/j.actbio.2016.10.018>.
- ⁷Dehghani, S., M. Rasoulianboroujeni, H. Ghasemi, S. H. Keshel, Z. Nozarian, M. N. Hashemian, M. Zarei-Ghanavati, G. Latifi, R. Ghaffari, Z. Cui, H. Ye, and L. Tayebi. 3D-Printed membrane as an alternative to amniotic membrane for ocular surface/conjunctival defect reconstruction: an in vitro & in vivo study. *Biomaterials.* 174:95–112, 2018. <https://doi.org/10.1016/j.biomaterials.2017.07.041>.
- ⁸Figueiredo, G. S., S. Bojic, P. Rooney, S. P. Wilshaw, C. J. Connon, R. M. Gouveia, C. Paterson, G. Lepert, H. S. Mudhar, F. C. Figueiredo, and M. Lako. Gamma-irradiated human amniotic membrane decellularised with sodium dodecyl sulfate is a more efficient substrate for the ex vivo expansion of limbal stem cells. *Acta Biomater.* 61:124–133, 2017. <https://doi.org/10.1016/j.actbio.2017.07.041>.
- ⁹Francisco, J., C. Ricardo, A. C. Marco, R. B. Simeoni, B. F. Mogharbel, L. P. Gledson, S. M. D. Dilcele, C.G.-S. Luiz, and C. Katherine. Decellularized amniotic membrane scaffold as a pericardial substitute: an in vivo study. *Transplant Proc.* 48(8):2845–2849, 2016. <https://doi.org/10.1016/j.transproceed.2016.07.026>.
- ¹⁰Frazão, L. P., J. Vieira de Castro, C. Nogueira-Silva, and N. M. Neves. Decellularized human chorion membrane as a novel biomaterial for tissue regeneration. *Biomolecules.* 10(9):1208, 2020. <https://doi.org/10.3390/biom10091208>.
- ¹¹Gholipourmalekabadi, M., M. Sameni, D. Radenkovic, M. Mozafari, M. Mossahebi-Mohammadi, and A. Seifalian. Decellularized human amniotic membrane: how viable is it as a delivery system for human adipose tissue-derived stromal cells? *Cell Prolif.* 49(1):115–121, 2016. <https://doi.org/10.1111/cpr.12240>.
- ¹²Gilbert, T. W., T. L. Sellaro, and S. F. Badylak. Decellularization of tissues and organs. *Biomaterials.* 27(19):3675–3683, 2006. <https://doi.org/10.1016/j.biomaterials.2006.02.014>.
- ¹³Go, Y. Y., S. E. Kim, G. J. Cho, S.-W. Chae, and J.-J. Song. Differential effects of amnion and chorion membrane extracts on osteoblast-like cells due to the different growth factor composition of the extracts. *PLoS ONE.* 12:e0182716, 2017. <https://doi.org/10.1371/journal.pone.0182716>.

- ¹⁴Grey, C., Tissue engineering scaffold fabrication and processing techniques to improve cellular infiltration. Dissertation, Virginia Commonwealth University, Richmond, 2014.
- ¹⁵Gupta, A., S. D. Kedige, and K. Jain. Amnion and chorion membranes: potential stem cell reservoir with wide applications in periodontics. *Int. J. Biomater.* 2015:1–9, 2015. <https://doi.org/10.1155/2015/274082>.
- ¹⁶Hamid, S., A. Muhammad, S. Zikria, I. Mehwish, I. Muhammad, D. Zeeshan, and K. Asif Manzoor. Mesenchymal stem cells (MSCs) as skeletal therapeutics—an update. *J. Biomed. Sci.* 23(41):1–15, 2016. <https://doi.org/10.1186/s12929-016-0254-3>.
- ¹⁷Jie, J., J. Yang, H. He, L. Zhang, Z. Li, J. Chen, M. Vimalin Jeyalatha, Z. Liu, and W. Li. Tissue remodeling after ocular surface reconstruction with denuded amniotic membrane. *Sci. Rep.* 8(1):6400, 2018. <https://doi.org/10.1038/s41598-018-24694-4>.
- ¹⁸Kakabadze, Z., K. Mardaleishvili, G. Loladze, I. Javakishvili, K. Chakhunasvili, L. Karalashvili, N. Sukhishvili, G. Chutkerashvili, A. Kakabadze, and D. Chakhunasvili. Clinical application of decellularized and lyophilized human amnion/chorion membrane grafts for closing post-laryngectomy pharyngocutaneous fistulas. *J. Surg. Oncol.* 113(5):538–543, 2016. <https://doi.org/10.1002/jso.24163>.
- ¹⁹Kannaiyan, J., S. Suriya-Narayanan, M. Palaniyandi, B. Rajangam, C. Hemlata, and P. Anubhav. Amniotic membrane as a scaffold in wound healing and diabetic foot ulcer: an experimental technique and recommendations. *IJRMS.* 2016. <https://doi.org/10.18203/2320-6012.ijrms20162206>.
- ²⁰Khalil, S., N. El-Badri, M. El-Mokhtaar, S. Al-Mofty, M. Farghaly, R. Ayman, H. Dina, and M. Noha. A cost-effective method to assemble biomimetic 3D cell culture platforms. *PLoS ONE.* 11(12):e0167116, 2016. <https://doi.org/10.1371/journal.pone.0167116>.
- ²¹Koob, T. J., J. J. Lim, M. Massee, N. Zabeck, R. Rennert, G. Gurtner, and W. W. Li. Angiogenic properties of dehydrated human amnion/chorion allografts: therapeutic potential for soft tissue repair and regeneration. *Vasc Cell.* 1(6):10, 2014. <https://doi.org/10.1186/2045-824X-6-10>.
- ²²Kshersagar, J., R. Kshirsagar, S. Desai, R. Bohara, and M. Joshi. Decellularized amnion scaffold with activated PRP: a new paradigm dressing material for burn wound healing. *Cell Tissue Bank.* 19(3):423–436, 2018. <https://doi.org/10.1007/s10561-018-9688-z>.
- ²³Lee, J. W., W. Y. Park, E. A. Kim, and I. H. Yun. Tissue response to implanted Ahmed glaucoma valve with adjunctive amniotic membrane in rabbit eyes. *Ophthalmic Res.* 51(3):129–139, 2014. <https://doi.org/10.1159/000357097>.
- ²⁴Li, X., L. Duan, Y. Liang, W. Zhu, J. Xiong, and D. Wang. Human umbilical cord blood-derived mesenchymal stem cells contribute to chondrogenesis in coculture with chondrocytes. *Biomed. Res. Int.* 2016:3827057, 2016. <https://doi.org/10.1155/2016/3827057>.
- ²⁵Lim, R. Concise review: fetal membranes in regenerative medicine: new tricks from an old dog? *Stem Cells Transl. Med.* 6(9):1767–1776, 2017. <https://doi.org/10.1002/sctm.16-0447>.
- ²⁶Litwiniuk, M., M. Radowicka, A. Krejner, A. Śladowska, and T. Grzela. Amount and distribution of selected biologically active factors in amniotic membrane depends on the part of amnion and mode of childbirth. Can we predict properties of amnion dressing? A proof-of-concept study. *Cent. Eur. J. Immunol.* 43(1):97–102, 2018. <https://doi.org/10.5114/cej.2017.69632>.
- ²⁷Maiti, S. K., M. U. Shiva Kumar, L. Srivastava, A. R. Ninu, and K. Naveen. Isolation, proliferation and morphological characteristics of bone-marrow derived mesenchymal stem cells (BM-MSC) from different animal species. *Trends Biomater. Artif. Organs.* 27(1):29–35, 2013.
- ²⁸Massee, M., K. Chinn, J. Lei, J. J. Lim, C. S. Young, and T. J. Koob. Dehydrated human amnion/chorion membrane regulates stem cell activity in vitro. *J. Biomed. Mater. Res. B Appl. Biomater.* 104(7):1495–1503, 2016. <https://doi.org/10.1002/jbm.b.33478>.
- ²⁹Massee, M., K. Chinn, J. J. Lim, L. Godwin, C. S. Young, and T. J. Koob. Type I and II diabetic adipose-derived stem cells respond in vitro to dehydrated human amnion/chorion membrane allograft treatment by increasing proliferation, migration, and altering cytokine secretion. *Adv. Wound Care (New Rochelle).* 5(2):43–54, 2016. <https://doi.org/10.1089/wound.2015.0661>.
- ³⁰McQuilling, J. P., J. B. Vines, K. A. Kimmerling, and K. C. Mowry. Proteomic comparison of amnion and chorion and evaluation of the effects of processing on placental membranes. *Wounds.* 29(6):E36–E40, 2017.
- ³¹Meller, D., V. Dabul, and S. C. Tseng. Expansion of conjunctival epithelium cells on amniotic membrane. *Exp. Eye Res.* 74:537–545, 2002. <https://doi.org/10.1006/exer.2001.1163>.
- ³²Mohammadi, A. A., S. M. Seyed Jafari, M. Kiasat, A. R. Tavakkolian, M. T. Imani, M. Ayaz, and H. R. Tolide-ie. Effect of fresh human amniotic membrane dressing on graft take in patients with chronic burn wounds compared with conventional methods. *Burns.* 39(2):349–353, 2013. <https://doi.org/10.1016/j.burns.2012.07.010>.
- ³³Monteiro, B. G., R. R. Loureiro, P. C. Cristovam, J. L. Covre, J. A. P. Gomes, and I. Kerkis. Amniotic membrane as a biological scaffold for dental pulp stem cell transplantation in ocular surface reconstruction. *Arq. Bras. Ophthalmol.* 82(1):32–37, 2019. <https://doi.org/10.5935/0004-2749.20190009>.
- ³⁴Naasani, L. S., A. F. Damo Souza, C. Rodrigues, S. Vedovatto, J. G. Azevedo, A. P. S. Bertoni, M. Da Cruz Fernandes, S. Buchner, and M. R. Wink. Decellularized human amniotic membrane associated with adipose derived mesenchymal stromal cells as a bioscaffold: physical, histological and molecular analysis. *Biochem. Eng.* 152:107366, 2019. <https://doi.org/10.1016/j.bej.2019.107366>.
- ³⁵Ngadiman, N. H. A., M. Y. Noordin, A. Idris, and D. Kurniawan. A review of evolution of electrospun tissue engineering scaffold: from two dimensions to three dimensions. *Proc. Inst. Mech. Eng. Part H J Eng. Med.* 231(7):597–616, 2017. <https://doi.org/10.1177/0954411917699021>.
- ³⁶Paolin, A., E. Cogliati, D. Trojan, C. Griffoni, A. Grassetto, H. M. Elbadawy, and D. Ponzin. Amniotic membranes in ophthalmology: long term data on transplantation outcomes. *Cell Tissue Bank.* 17(1):51–58, 2016. <https://doi.org/10.1007/s10561-015-9520-y>.
- ³⁷Parry, S., and J. F. Strauss III. Premature rupture of the fetal membranes. *N. Engl. J. Med.* 338(10):663–670, 1998. <https://doi.org/10.1056/NEJM199803053381006>.
- ³⁸Porzionato, A., E. Stocco, S. Barbon, F. Grandi, V. Macchi, and R. De Caro. Molecular sciences tissue-engineered grafts from human decellularized extracellular matrices: a

- systematic review and future perspectives. *IJMS*. 19(12):4117, 2018. <https://doi.org/10.3390/ijms19124117>.
- ³⁹Rana, D., S. Arulkumar, A. Vishwakarma, and M. Ramalingam. Considerations on Designing Scaffold for Tissue Engineering. *Stem Cell Biology and Tissue Engineering in Dental Sciences*. New York: Academic Press, pp. 133–148, 2015.
- ⁴⁰Rao Pattabhi, S., J. S. Martinez, and T. C. Keller 3rd. Decellularized ECM effects on human mesenchymal stem cell stemness and differentiation. *Differentiation*. 88(4–5):131–143, 2014. <https://doi.org/10.1016/j.diff.2014.12.005>.
- ⁴¹Rieder, E., M.-T. Kasimir, G. Silberhumer, G. Seebacher, E. Wolner, P. Simon, and G. Weigel. Decellularization protocols of porcine heart valves differ importantly in efficiency of cell removal and susceptibility of the matrix to recellularization with human vascular cells. *J. Thorac. Cardio. Surg.* 127(2):399–405, 2004. <https://doi.org/10.1016/j.jtcvs.2003.06.017>.
- ⁴²Saghizadeh, M., M. A. Winkler, A. A. Kramerov, D. M. Hemmati, C. A. Ghiam, S. D. Dimitrijevic, D. Sareen, L. Ornelas, H. Ghiasi, W. J. Brunken, E. Maguen, Y. S. Rabinowitz, C. N. Svendsen, K. Jirsova, and A. V. Ljubimov. A simple alkaline method for decellularizing human amniotic membrane for cell culture. *PLoS ONE*. 8(11):e79632, 2013. <https://doi.org/10.1371/journal.pone.0079632>.
- ⁴³Salah, R. A., I. K. Mohamed, and N. El-Badri. Development of decellularized amniotic membrane as a bioscaffold for bone marrow-derived mesenchymal stem cells: ultrastructural study. *J. Mol. Histol.* 49(3):289–301, 2018. <https://doi.org/10.1007/s10735-018-9768-1>.
- ⁴⁴Sara, L. M., K. Thomas, H. Nicola, P. Olena, F. Carsten, B. Martin, F. Constanca, G. Birgit, and G. Oleksandr. Human amniotic membrane: a review on tissue engineering, application, and storage. *J. Biomed. Mater. Res. B Appl. Biomater.* 2021:1–18, 2020. <https://doi.org/10.1002/jbm.b.34782>.
- ⁴⁵Schenke-Layland, K. From tissue engineering to regenerative medicine—the potential and the pitfalls. *Adv. Drug Deliv. Rev.* 63(4–5):193–194, 2011. <https://doi.org/10.1016/j.addr.2011.04.003>.
- ⁴⁶Strauss, J. F., 3rd. Extracellular matrix dynamics and fetal membrane rupture. *Reprod. Sci.* 20(2):140–153, 2013. <https://doi.org/10.1177/1933719111424454>.
- ⁴⁷Taghiabadi, E., S. Nasri, S. Shafieyan, S. J. Firoozinezhad, and N. Aghdami. Fabrication and characterization of spongy denuded amniotic membrane based scaffold for tissue engineering. *Cell J.* 16(4):476–487, 2015. <https://doi.org/10.22074/cellj.2015.493>.
- ⁴⁸Tiziana, S., P. Gianfranco, and G. Umberto. Clinical trials with mesenchymal stem cells: an update. *Cell Transplant.* 25(5):829–848, 2016. <https://doi.org/10.3727/096368915x689622>.
- ⁴⁹Wang, M., Y. Yang, D. Yang, F. Luo, W. Liang, S. Guo, and J. Xu. The immunomodulatory activity of human umbilical cord blood-derived mesenchymal stem cells in vitro. *Immunology.* 126(2):220–232, 2009. <https://doi.org/10.1111/j.1365-2567.2008.02891.x>.
- ⁵⁰Wilshaw, S. P., J. N. Kearney, J. Fisher, and E. Ingham. Production of an acellular amniotic membrane matrix for use in tissue engineering. *Tissue Eng.* 12:2117–2129, 2006. <https://doi.org/10.1089/ten.2006.12.2117>.
- ⁵¹Wilshaw, S. P., J. Kearney, J. Fisher, and E. Ingham. Biocompatibility and potential of acellular human amniotic membrane to support the attachment and proliferation of allogeneic cells. *Tissue Eng. Part A.* 14:463–472, 2008. <https://doi.org/10.1089/tea.2007.0145>.
- ⁵²Yang, S., K.-F. Leong, Z. Du, and C.-K. Chua. The design of scaffolds for use in tissue engineering. Part I. Traditional factors. *Tissue Eng.* 7(6):679–689, 2001. <https://doi.org/10.1089/107632701753337645>.
- ⁵³Zare-Bidaki, M., S. Sadrinia, S. Erfani, E. Afkar, and N. Ghanbarzade. Antimicrobial properties of amniotic and chorionic membranes: a comparative study of two human fetal sacs. *J. Reprod. Infertil.* 18(2):218–224, 2017.

Publisher's Note Springer Nature remains neutral with regard to jurisdictional claims in published maps and institutional affiliations.